

A Complete LoRaWAN Model for Single-Gateway Scenarios

Davide Magrin, *Student Member, IEEE*, Martina Capuzzo, *Student Member, IEEE*,
Andrea Zanella, *Senior Member, IEEE*, and Michele Zorzi, *Fellow, IEEE*

Abstract—LoRaWAN is a Low Power Wide Area Network technology featuring long transmission range and a simple MAC layer that have favored its adoption and usage in large-scale deployments. While LoRaWAN’s main use case consists in unconfirmed sensor data collection, the standard also considers confirmed traffic, enabling control applications and reliable services. Although this feature does have important implications in terms of system settings and performance, it has mostly been overlooked in the literature. To contribute filling this gap, in this paper we provide a mathematical model to estimate the performance of a LoRaWAN gateway serving a set of devices that may employ confirmed traffic. The model also features a set of parameters that can be adjusted to investigate different behaviors of the gateway, making it possible to carry out a systematic analysis of various trade-offs. The accuracy of the proposed model is validated against ns-3 LoRaWAN simulations.

I. INTRODUCTION

The Internet of Things (IoT) promises to be a disruptive paradigm that will change our everyday activities, offering smart solutions in which remote monitoring and control of potentially every object is enabled through an Internet connection. The paradigm foresees multiple applications in a wide variety of scenarios: from fleet tracking and process monitoring in industrial scenarios to smarter garbage collection and intelligent light control in cities; from monitoring of soil moisture in agriculture to home temperature control and personal health monitoring [1], [2], [3].

The presence of several use cases spawned an ample market, and encouraged the development of multiple technologies meeting the need for low cost ubiquitous connectivity. A large part of IoT nodes will largely consist in monitoring sensors that generate sporadic traffic, without strict constraints in terms of latency and throughput. This calls for new wireless solutions that have to support a massive number of devices, with an affordable cost for both user equipment and network infrastructure. Therefore high energy efficiency, extended coverage, and infrastructure simplicity are aspects of primary importance.

Such requirements motivated the creation of a new family of wireless technologies collectively called Low Power Wide Area Networks (LPWANs), characterized by long coverage range and low power consumption. A prominent LPWAN technology is LoRaWAN, which claims up to 10 years battery

The authors are with the Dept. of Information Engineering (DEI), University of Padova, Via Gradenigo 6/b, 35131 Padova, Italy. Prof. A. Zanella is also with the Human Inspired Technology (HIT) center, of the University of Padova. Email: {magrinda, capuzzom, zanella, zorzi}@dei.unipd.it

lifetime for devices, and a transmission range between 1.5 km in urban scenarios and 30 km in rural areas.

Since the deployment of a dense IoT network is expensive and time consuming, performance assessments using simulations and mathematical models become essential to gauge the effect of network parameters and estimate the performance at a reduced cost.

In this work we propose an analytical model of the performance of a LoRaWAN network, accounting for both the Physical (PHY) and Medium Access Control (MAC) layer specificities of the technology. The proposed model can be configured to assess the impact of several network parameters, such as the distribution of the Spreading Factors (SFs) and the Gateway (GW) configuration, as well as the effect of regional regulations such as the Duty Cycle (DC) limitations. Furthermore, the mathematical model takes into account the fact that a portion of the devices in the network might generate confirmed traffic and re-transmit their message if no Acknowledgment (ACK) is received from the GW.

The rest of this work is structured as follows. In Sec. II and Sec. III we present the LoRaWAN technology, and give an overview of the current state of the art in LoRaWAN evaluation and modeling, respectively. Sec. IV introduces the proposed model and the set of parameters that can be tuned, while Sec. V provides the mathematical description of the model. Model validation and further insights are provided in Sec. VI. Finally, Sec. VII draws the conclusions and discusses possible future developments.

II. TECHNOLOGY OVERVIEW

This section describes the key LoRaWAN features, introducing the modulation it is based on and explaining the main aspects of the standard at the MAC layer. The discussion will also present elements and properties that have a significant impact on the system-level performance, and that will be then considered in the model formulation.

A. The LoRa modulation

LoRa is a modulation technique based on chirp spread spectrum, patented by Semtech. The modulation can be tuned using the SF parameter that directly influences data rate and coverage range and that can vary from 7 to 12. Lower SF values can achieve a higher data rate and shorter transmission times, but require higher signal powers at the receiver for correct decoding, which implies shorter coverage ranges. On the other hand, signals transmitted using higher SFs are

more robust to channel impairments and can achieve longer distances, at the price of an increased transmission time due to lower data rates. Furthermore, signals modulated with different SFs are almost orthogonal: even if overlapping in time and frequency, two or more signals transmitted with different SFs can be simultaneously decoded, provided that their received powers satisfy some conditions [4].

B. The LoRaWAN standard

The LoRaWAN standard considers a star topology with three kinds of devices:

- the *Network Server (NS)*, which is the central network controller and can be located anywhere in the Internet;
- the *End Devices (EDs)*, that are peripheral nodes, usually sensors or actuators that transmit using the LoRa modulation;
- the *Gateways (GWs)*, i.e., relay nodes that collect messages from the EDs through the LoRa interface, and forward them to the NS using a legacy IP connection, and *vice versa*.

The standard also defines three classes of EDs, which differ for the time they spend in reception mode. This article considers the most common *Class A* devices, which have the strictest requirements in terms of energy consumption. In order to save battery, these devices stay in sleep mode for most of the time, opening two reception windows only 1 and 2 seconds after the end of the Uplink (UL) packet transmission. The EDs have the possibility of transmitting *unconfirmed* or *confirmed* packets: in the second case, an ACK is expected in one of the two reception opportunities after the transmission to confirm the correct reception of the packet by the NS.¹ If the ACK is not received in any of the two reception windows, a re-transmission is performed. The same message can be transmitted up to m times, and is dropped if all these attempts fail. The value of m can be configured by the NS. It is worth noting that, when unconfirmed packets are sent, the reception windows are opened even if no ACK is expected, since these time slots are the only opportunities for the NS to communicate with the EDs.

The UL messages transmitted by an ED are collected by all the GWs in the coverage range of the transmitter, and forwarded to the NS. If the ED requires a reply, the NS can pick any of these GWs to transmit the DL message.

The standard also defines the frequency bands, power and DC restrictions that apply to the different regions. Table I shows the configuration mandated for the European region which entails three bidirectional channels and a fourth channel reserved to DL transmissions only. The 868.1, 868.3, 868.5 MHz channels belong to the same frequency band, and have to share a DC limitation of 1%, while the channel reserved for the DL can benefit from a more lenient DC of 10% and a higher transmission power.

By native-settings, EDs open the first receive window (RX1) on the same frequency channel of the UL transmission, and

¹Although in this paper we focus on ACK transmissions, the model and the analysis hold for any Downlink (DL) packet returned by the NS to the ED after the reception of a UL packet by the NS.

Table I
AVAILABLE LoRAWAN CHANNELS

Frequency [MHz]	Use	Duty Cycle
868.1	UL/DL	1%, shared
868.3	UL/DL	1%, shared
868.5	UL/DL	1%, shared
869.525	DL	10%, dedicated

expect a signal modulated with the same SF. The second receive window (RX2), instead, is opened on the 869.525 MHz channel and the incoming signal is assumed to use SF 12, to maximize the coverage rate. In Sec. VI we will present the effects of changing the SF used in RX2. The standard, in fact, allows the NS to modify this pre-defined configuration by communicating the new settings to the ED through appropriate MAC commands.

The GW chipset, described in [5], provides 8 reception chains that need to be configured to listen to a certain frequency, and can decode signals with any SF. GWs do not support full-duplex transmission: to send a DL packet they have to interrupt any ongoing reception.

C. Packet life cycle

Messages transmitted by EDs to the GW are subject to multiple causes of losses:

- *Interference*: packets sent in the same frequency channel and with the same SF collide. A transmission can survive a collision event if its received power is sufficiently higher than that of the other overlapping signals.
- *GW already in transmission*: the GW can not lock on a UL packet when it is performing a DL transmission.
- *GW starting a transmission*: an ongoing packet reception may be interrupted if the GW needs to send a DL packet. The UL message is therefore lost.

Moreover, confirmed UL messages cause the NS to generate ACKs that need to be transmitted by the GW. Such DL transmissions may as well be impaired by a number of events:

- *Unavailability of receive windows*: this event occurs when both the receive windows in all available GWs are unavailable because of the DC constraint or other ongoing transmissions.
- *Interference*: DL packets transmitted in RX1 can collide with UL packets transmitted in the same channel by other EDs.

In this work, we provide a network model that accounts for all these events.

III. STATE OF THE ART IN LoRAWAN MODELING

To date, the literature has been mainly focused on the performance analysis of LoRaWAN networks employing UL-only communication, with only a few exceptions. For example, the authors of [6], [7], [8], leverage the ns-3 simulator to extract metrics for both confirmed and unconfirmed traffic. A similar investigation is conducted in [9], which adds ACKs and re-transmissions to the Python-based LoRaSim simulator. The

authors of [10], instead, rely on a custom MATLAB simulator and tune the network parameters based on the requirements of an actual metering application. Generally, these works identify DL traffic as a weak point in the LoRaWAN technology, because of either the strict DC limitations in Europe or its deleterious effect on UL traffic, and point to GW densification as a partial solution to the problem.

Mathematical analysis has also been used to assess various network performance metrics. In [11], the authors address high-level questions about LoRaWAN's suitability for a range of smart city applications, from metering to video surveillance, by modeling the system as a superposition of different Aloha networks. The work presented in [12] is one of the first to address the issue of scalability, using stochastic geometry to model interference in a LoRaWAN network. However, the study considers scenarios with only UL traffic. The work in [13] adopts a Markovian approach to model the over-the-air activation procedure, while [14] focuses on the energy consumption of LoRa radio chips. In [15] instead, queueing theory is applied to model latency and throughput of an ED subject to DC constraints, again focusing on UL communication. Finally, the authors of [16], [17] provide a model based on Poisson arrival processes that takes DL communications and re-transmissions into account. However the analysis holds only in limited-size networks, where nodes can employ any Modulation and Coding Scheme (MCS) and their received powers are similar.

The work presented in this paper is an extension of our previous conference paper [18], where we modeled packet arrivals as a Poisson process, and included the DC limitations of European deployments and a set of network parameters. The study presented here is based on a novel approach to accurately describe the behavior of the receive windows and their usage under DC constraints. Additionally, we include the presence of packet re-transmissions and the coexistence of unconfirmed and confirmed traffic, and at the same time keep the possibility of tuning other network configuration settings. This article also presents a comparison of the results obtained through this model with those given by the LoRaWAN simulator presented in [19], further attesting the accuracy of the proposed approach.

IV. MODEL: PRELIMINARY CONSIDERATIONS

The aim of the model proposed in this paper is to characterize the behavior of a LoRaWAN network at the level of a single GW, which is receiving packets from a set of EDs and needs to reply in one of the two receive windows if the ED requires confirmation. Performance is described in terms of packet success probability, following the approach used in [18] and extending it with a better characterization of the GW behavior. In the following we describe the reference scenario and the model assumptions. Furthermore, we detail the system parameters that can be set. Then, we provide an overview of the mathematical concepts that are at the basis of the model. The mathematical details are developed in Sec. V.

A. Scenario and assumptions

We consider a scenario where the EDs are randomly and uniformly distributed around a single GW. We assume that each device can transmit only one type of message, either confirmed or unconfirmed. Packets are generated at the application level following independent Poisson processes with aggregate packet generation rate λ .

For tractability, we assume perfect orthogonality between different SFs, i.e., only packets employing the same SF can collide and, in this case, they are both lost. While this assumption has been shown to have an impact on the PHY-layer performance of UL only traffic [4], the results discussed in Sec. VI show that the effect is much more limited in the presence of confirmed traffic.

B. System parameters

Our model presents some settable parameters to increase its flexibility, enabling the evaluation of the network performance in various configurations with minimum effort. More specifically, the model makes it possible to specify the following values.

- p_i : probability that a UL message is transmitted with SF i .
- α : fraction of devices using confirmed traffic. Therefore, the application-layer packet generation rate for confirmed messages will be $\alpha\lambda$, while that for unconfirmed messages will be $(1 - \alpha)\lambda$.
- m : maximum number of transmission attempts.
- δ : DC limitation flag. We set $\delta=1$ if the DC constraint at the GW is enabled. Instead, we set $\delta=0$ if the GW is not subject to any DC constraint, a possibility that is actually not permitted by European regulations but that we consider for the sake of scientific exploration.
- τ : prioritization flag. If $\tau = 0$, the reception operations are prioritized over transmission at the GW. In this case, the GW will drop any DL message that needs to be transmitted while a UL reception is ongoing. Instead, if TX is prioritized ($\tau = 1$), the reception of any incoming packet will be interrupted in order to send the ACK.
- F : number of UL frequency channels.
- T_x^{ack2} : transmission time of the ACK in RX2 when using SF x . (The standard considers packets transmitted in RX2 to use SF 12 as pre-configured setting, corresponding to T_{12}^{ack2}).
- Number of ACKs that the GW will attempt to send in response to each UL confirmed packet: either just one ACK in one of the receive windows according to their availability (as in the LoRaWAN standard), or two using both receive windows whenever possible (in an attempt to make ACK delivery more reliable).

C. Model rationale

Fig. 1 depicts an example of the packet reception model, consisting in successive filtering of Poisson processes. At the base of the figure, arrows are used to represent the UL traffic generated by the EDs, including both new packet transmissions and re-transmissions of failed packets. This process

is assumed to be Poisson for tractability, ignoring the fact that re-transmissions of a same packet have a fixed period because of DC limitations and thus are correlated in time. An initial filtering of this process excludes some arrivals, modeling packet losses due to interference from other EDs or ongoing DL transmissions from the GW. This yields a process with a reduced rate, which now represents packets that are correctly received by the GW.

When the received UL message requires a confirmation, an ACK must be sent by the GW during one of the two receive windows of the target ED. The ability of the GW to perform such a transmission is modeled through two independent alternating renewal processes, in which the system alternates between an ON state, representing the fact that the GW is available to send a reply in that window, and an OFF state, where ACK sending is prevented by another ongoing transmission or DC constraints. When the GW becomes available for transmission again, the process switches back to the ON state. Since the two receive windows operate on different sub-bands, we assume that the two processes are uncorrelated, neglecting the fact that the packets that need to be served in RX2 are those that found RX1 in the OFF state. If the DL packet finds at least one of the two processes in the ON state, an ACK is sent. If the ACK is sent on RX1 (hence, using frequencies shared by UL and DL traffic), it gets correctly received by the ED unless it is destroyed by the interference created by other EDs.

For the sake of clarity, the following list describes the life cycle of the packets in Fig. 1:

- (A) This packet is lost because of interference or GW transmission. Hence, it does not pass the first filter.
- (B) This is an unconfirmed UL packet, which is successfully received by the GW. It does not generate any ACK.
- (C) This is a confirmed packet successfully received by the GW. It generates an ACK, which finds RX1 in the ON state. The ACK is successfully sent, and the RX1 process switches to the OFF state.
- (D) This is another confirmed packet which is successfully received by the GW. Since the GW has just sent an ACK for packet (C), it cannot reply in RX1 due to DC constraints; RX2 is however in the ON state, and the GW can thus reply to the ED, making the second process switch to the OFF state.
- (E) This is another confirmed packet, which gets a treatment similar to that of packet (D). However, since the GW has transmitted the ACK for packet (D) and is still under the DC constraints, it cannot reply to packet (E) in any of the two receive windows (both RX1 and RX2 processes are in the OFF state). The DL packet is hence discarded, and the ED will re-transmit the UL message at a later time.

V. MODEL

In this section we provide the mathematical formulation of the model. In addition to the parameters introduced in Sec. IV-B, we call \mathcal{S} the set of possible spreading factors, while T_i^{data} and T_i^{ack1} are the time durations of a data packet and of an ACK transmitted in RX1 with SF i , respectively.

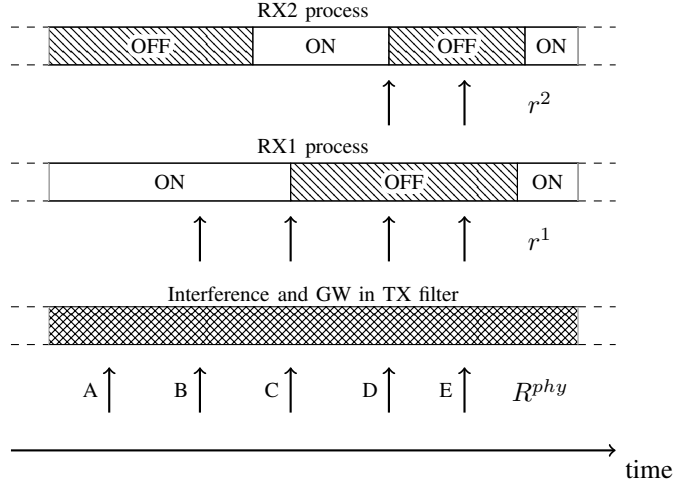


Figure 1. Representation of the model's packet filtering structure.

Moreover, we indicate with T_i^{ack2} the time-on-air of an ACK sent in RX2. Note that, with the standard's configuration, ACKs transmitted in RX2 always use SF 12, irrespective of the SF employed in the UL transmission: in this case, therefore, $T_i^{ack2} = T_{12}^{ack} \forall i \in \mathcal{S}$. On the other hand, if the DL packet is sent in RX2 using the same SF employed in RX1 (as also permitted in our model), we set $T_i^{ack2} = T_i^{ack1}$.

A. Uplink traffic rates

The assumption of perfect orthogonality between different SFs makes it possible to split the network traffic in different logical channels that do not interfere with each other. The traffic load for each SF i is assumed to be split uniformly over the given F frequency channels, and is given by:

$$R_i^{app} = \frac{p_i \cdot \lambda}{F}, i \in \mathcal{S}. \quad (1)$$

The traffic generated at the application layer by the EDs using confirmed and unconfirmed messages is, respectively, given by:

$$R_i^{c,app} = R_i^{app} \cdot \alpha, \quad (2)$$

$$R_i^{u,app} = R_i^{app} \cdot (1 - \alpha). \quad (3)$$

Since EDs using unconfirmed traffic do not perform any re-transmission, the traffic injected in the network by these devices at the PHY level is equal to that generated by the application, i.e., $R_i^{u,phy} = R_i^{u,app}$.

For EDs transmitting confirmed messages, instead, the re-transmitted packets generated after a missing ACK must also be considered. We indicate as $P_i^{DL}(j)$ the probability that a confirmed UL packet sent with SF i is successfully received and acknowledged at the j -th transmission attempt. Therefore, we have that the total packet rate of confirmed traffic is given by the product of the application-level rate and the average number of times that a confirmed packet is transmitted at the PHY layer, i.e., :

$$R_i^{c,phy} = R_i^{c,app} \left[\sum_{j=1}^m j P_i(j) + m \left(1 - \sum_{j=1}^m P_i(j) \right) \right]. \quad (4)$$

The total traffic for a single frequency channel and for SF i is therefore given by:

$$R_i^{phy} = R_i^{u,phy} + R_i^{c,phy}. \quad (5)$$

B. PHY layer probabilities

As already explained, a UL packet is successfully received by the GW if: (i) it does not overlap with another UL transmission using the same SF, and (ii) it does not occur during a GW DL transmission. This is represented by the first filter in Fig. 1.

Since packets are generated following a Poisson process, the probability of the first event is given by

$$S_i^{INT} = e^{-2T_i^{data} R_i^{phy}}, \quad (6)$$

which is the probability that there are no arrivals during the $2T_i^{data}$ vulnerability period.

The probability of the second event can be computed as the ratio between the time interval during which the reception of a UL message is disrupted by the transmission of ACKs, and the average duration of an ON-OFF cycle. For the numerator, we observe that a UL message is always lost when it arrives at the GW during the transmission of an ACK. Otherwise, the GW will start the reception of the UL message, which will take a time T_i^{data} . If $\tau = 0$, the reception cannot be interrupted, and the UL message will be successfully delivered to the NS. Conversely, if $\tau = 1$, the reception of the UL packet may be aborted at any time during the period T_i^{data} , in order to give priority to an ACK transmission. Therefore, the vulnerability period is given by the ACK transmission time, which is preceded by an interval of T_i^{data} to be accounted for only if $\tau = 1$. Now, according to the *Poisson Arrivals See Time Averages* (PASTA) property, the probability that a UL packet arrival falls in the vulnerability period for the receive window RX k , with $k = 1, 2$, can be expressed as

$$F_i^{TXk} = \frac{\sum_{s \in S} d_s T_s^{ack_k} + T_i^{data} \cdot \tau}{E_{ONk} + E_{OFFk}}, \quad (7)$$

where the denominator is the mean renewal time of the RX k process (i.e., the average duration of an ON-OFF cycle), while the numerator is the mean vulnerability period. Note that $\{d_s\}$ denotes the probability that an ACK is transmitted with SF $s \in S$, which will be derived later. Then, assuming once again that the events in RX1 and RX2 channels are independent, the probability that a UL packet reception is successful can then be expressed as

$$S_i^{TX} = (1 - F_i^{TX1})(1 - F_i^{TX2}), \quad (8)$$

and the overall UL packet success probability is finally expressed as

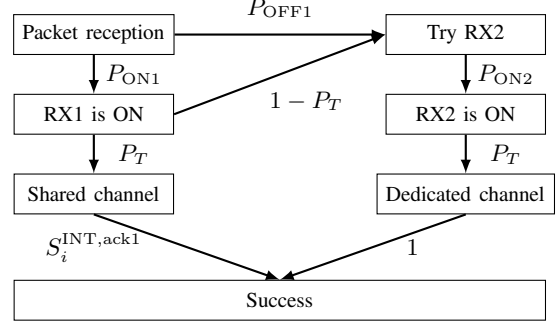


Figure 2. Diagram for ACK generation.

$$S_i^{UL} = S_i^{INT} \cdot S_i^{TX}. \quad (9)$$

In turn, the arrival rate of confirmed messages to the GW can be expressed as

$$r_i^1 = R_i^{c,phy} \cdot S_i^{UL}. \quad (10)$$

From this quantity we can finally derive the probability distribution $\{d_i\}$ of the SF used for ACK transmissions, which is given by:

$$d_i = \frac{r_i^1}{\sum_{i \in S} r_i^1}. \quad (11)$$

C. ACK transmission

Once a confirmed packet is correctly received by the GW, an ACK needs to be transmitted back to the ED. A visual representation of the possible ACK life cycle considered in the model is shown in Fig. 2. The labels refer to the probabilities of the different events, which are derived in the following. In general, an ACK is transmitted if both the following conditions hold: (a) $\tau = 1$ or $\tau = 0$ and the GW is idle; (b) either RX1 or RX2 is available (i.e., not blocked by DC constraints). If either condition is not satisfied, the ACK is dropped.

Let T denote the event (a), i.e., “the GW may transmit,” which depends on the TX/RX prioritization policy. If $\tau = 1$, the GW can transmit the DL packet whenever it needs to; otherwise, if $\tau = 0$, the GW can transmit only if no reception is ongoing. We denote by P_T the probability of such event, which can be computed as

$$P_T = \begin{cases} 1, & \text{if } \tau = 1; \\ e^{-\sum_{i \in S} F \cdot R_i^{phy} T_i^{data}}, & \text{if } \tau = 0; \end{cases} \quad (12)$$

where the second expression is the probability that no UL packet is generated in the last T_i^{data} seconds.

If RX1 is not available, the ACK will be handed to RX2. Such packets form a Poisson process with rate:

$$r_i^2 = r_i^1 [P_{OFF1} + P_{ON1}(1 - P_T)], \quad (13)$$

where P_{ON1} and P_{OFF1} are the probabilities of finding RX1 in the ON and OFF state, respectively, and $(1 - P_T)$ is the probability that the GW is not available for DL transmission. The ON and OFF probabilities for the RX k process, with $k = 1, 2$, are given by

$$P_{ONk} = \frac{E_{ONk}}{E_{ONk} + E_{OFFk}}, \quad (14)$$

$$P_{OFFk} = \frac{E_{OFFk}}{E_{ONk} + E_{OFFk}}, \quad (15)$$

where E_{ONk} and E_{OFFk} are the expected times the RX k process spends in the ON and OFF states, respectively, during a renewal period (ON-OFF cycle).

By considering the arrival rate of successful UL packets we have:

$$E_{ONk} = \frac{1}{\sum_{i \in \mathcal{S}} F \cdot r_i^k}. \quad (16)$$

Note that the switch from the ON to the OFF state will be caused by a packet sent in any of the F UL channels: therefore, we need to multiply the per-frequency rates r_i^1 and r_i^2 by the number of available channels.

In our model, the OFF period accounts for the time to send the ACK using the given SF, plus the waiting time imposed by the DC limitations. We hence have

$$\begin{aligned} E_{OFF1} &= \sum_{i \in \mathcal{S}} d_i (T_i^{ack1} + 99T_i^{ack1} \cdot \delta), \\ E_{OFF2} &= \sum_{i \in \mathcal{S}} d_i (T_i^{ack2} + 9T_i^{ack2} \cdot \delta). \end{aligned} \quad (17)$$

where the 99 and 9 values correspond to the duty cycle limitations of 1% and 10% on the channels used for RX1 and RX2, respectively.

Note that, by including the parameter δ as defined in Sec. IV-B, we consider the possibility of turning off the DC limitations.

D. Computation of success probabilities

DL packets sent by the GW in RX1 also have to avoid interference from other EDs. Here, the vulnerability period is given by the sum of the time on air of the data and ACK packets. Therefore, the probability that the ACK does not collide with a UL packet in RX1 is equal to

$$S_i^{INT,ack1} = e^{-R_i^{phy}(T_i^{data} + T_i^{ack1})}. \quad (18)$$

For packets sent in RX2, instead, the reception is assumed to always be successful, since the 869.525 MHz channel is dedicated to DL communication and the GW only transmits one packet at a time (this assumption does not hold in the case of multiple GWs).

Putting all the pieces together, we express the DL success probability when one ACK is used as:

$$\begin{aligned} S_i^{DL} &= P_{ON1} \cdot P_T \cdot S_i^{INT,ack1} + \\ &[P_{OFF1} + P_{ON1} \cdot (1 - P_T)] \cdot P_{ON2} \cdot P_T, \end{aligned} \quad (19)$$

where the first term describes the probability of a successful ACK transmission in RX1, while the second term accounts for the probability that RX1 is not available, and the ACK is successfully sent on RX2. Fig. 2 can be used as a reference for the computation of this quantity.

In case two ACKs are employed, one for each receive window, the expression of the probability of successful ACK transmission becomes:

$$\begin{aligned} S_i^{DL} &= P_{ON1} \cdot P_T \cdot S_i^{INT,ack1} + \\ &P_{ON2} \cdot P_T - \\ &P_{ON1} \cdot P_T \cdot P_{ON1} \cdot P_T \cdot S_i^{INT,ack1}, \end{aligned} \quad (20)$$

where we compute the probability that either RX1, or RX2, or both transmission attempts are successful.

Finally, we can compute the success probabilities over m transmissions. We remark that, although re-transmissions of a packet are correlated in time due to DC constraints, we assume them to be independent for simplicity (the accuracy of this approximation will be verified by simulation). We call $P_i^{UL}(j)$ the probability that a UL packet is successfully received at the GW at exactly the j -th transmission attempt, which is computed as:

$$P_i^{UL}(j) = S_i^{UL} [1 - S_i^{UL}]^{j-1}. \quad (21)$$

Then, we denote by $P_i(j)$ the probability that the ED successfully receives the ACK at exactly the j -th attempt, that can be expressed as

$$P_i(j) = [1 - (S_i^{UL} S_i^{DL})]^{j-1} \cdot (S_i^{UL} S_i^{DL}). \quad (22)$$

We hence have a set of cross-referential equations (1) – (22), whose solution can be found with iterative search methods.

E. Performance metrics

Network performance can be evaluated in terms of Packet Delivery Rate (PDR). According to the specific use case, three definitions of this metric are given:

- *Unconfirmed Uplink PDR (UU)*: fraction of unconfirmed packets that are successfully received by the GW;
- *Confirmed Uplink PDR (CU)*: fraction of (application-layer) confirmed packets that are successfully received by the GW, irrespective of whether the corresponding ACK is successfully received by the ED;
- *Confirmed Downlink PDR (CD)*: fraction of (application-layer) confirmed packets that are successfully acknowledged by the NS.

Clearly, $CD \leq CU$, since a packet needs to be successfully received by the GW in order to be acknowledged. Note that the CU metric captures the performance of applications for which it is important to deliver packets to the NS and ACKs are only used to stop re-transmissions (and thus avoid a useless increase in traffic), while CD is more interesting for applications that require the EDs to get explicit feedback from the NS, for instance containing control information addressed to the ED.

We obtain the UU and CU values by averaging the UL success probability for each SF over the SF distribution, i.e., :

$$UU = \sum_{i \in \mathcal{S}} p_i \cdot S_i^{UL}, \quad (23)$$

$$CU = \sum_{i \in \mathcal{S}} \left(p_i \cdot \sum_{j=1}^m P_{i,j}^{UL} \right). \quad (24)$$

Similarly, CD is computed as the probability of success within the available re-transmission attempts:

$$CD = \sum_{i \in S} \left(p_i \cdot \sum_{j=1}^m P_{i,j}^{DL} \right). \quad (25)$$

VI. RESULTS

To validate the model with simulation results, we first set some of the parameters described in Sec. IV-B.

SF distribution – EDs are assigned the minimum SF such that their received power at the GW, which depends on the propagation channel, is above the sensitivity threshold for that SF. We consider an open-air environment with only path loss, since the fast-fading component is supposed to be averaged out by the LoRa modulation. Hence, we follow the log distance propagation loss model also employed in [19]. The EDs are located in a circular area of 6.3 km radius, such that they are all in range of the GW when using SF 12. As a consequence, the distribution of the SFs only depends on the distance between the ED and the GW, resulting in concentric annuli of devices using the same SF, where the employed SF increases with the distance from the GW.

Channel allocation – We consider the typical frequency allocation scheme in Europe, as reported in Tab. I. Therefore, the number of different frequency channels for UL is $F = 3$.

Variable parameters – We study the network performance for different values of α , spanning from the case where all EDs transmit confirmed traffic ($\alpha = 1$) to the case where only unconfirmed traffic is generated ($\alpha = 0$). We also explore the impact of different values of m , of the TX and RX prioritization ($\tau = 0, 1$), and of the usage of a fast data rate in RX2, as opposed to the default usage of SF 12.

Fixed parameters – In this work, we do not show the effect of some non-standard settings that the model can include (e.g., double ACK, disabling of DC limitations). The impact of these parameters was studied by simulation in [20].

In the following, we discuss a selection of results that can be obtained from the proposed model, first comparing them with simulation results and then showing how they can provide insights about the behavior of the network.

Simulation results have been obtained by using the lorawan module of the ns-3 simulator, described in [19] and [6]. The simulator strives to be as realistic as possible, and also takes into account some factors that are overlooked by the model for tractability reasons. Transmissions employing different SFs, for instance, are not assumed to be perfectly orthogonal, rather the simulator relies on the link-level model provided in [21], which also accounts for the capture effect. Differently from the model, simulated LoRaWAN nodes also experience path loss, so that farther devices will be penalized with respect to EDs that are close to the GW. Finally, a realistic model is employed for the GW chipset [5], which entails a maximum of 8 parallel receptions paths, as described in Sec. II.

A first comparison between the results given by the simulator and the model is provided in Fig. 3. The figure shows the CU and CD metrics for a network in which all EDs

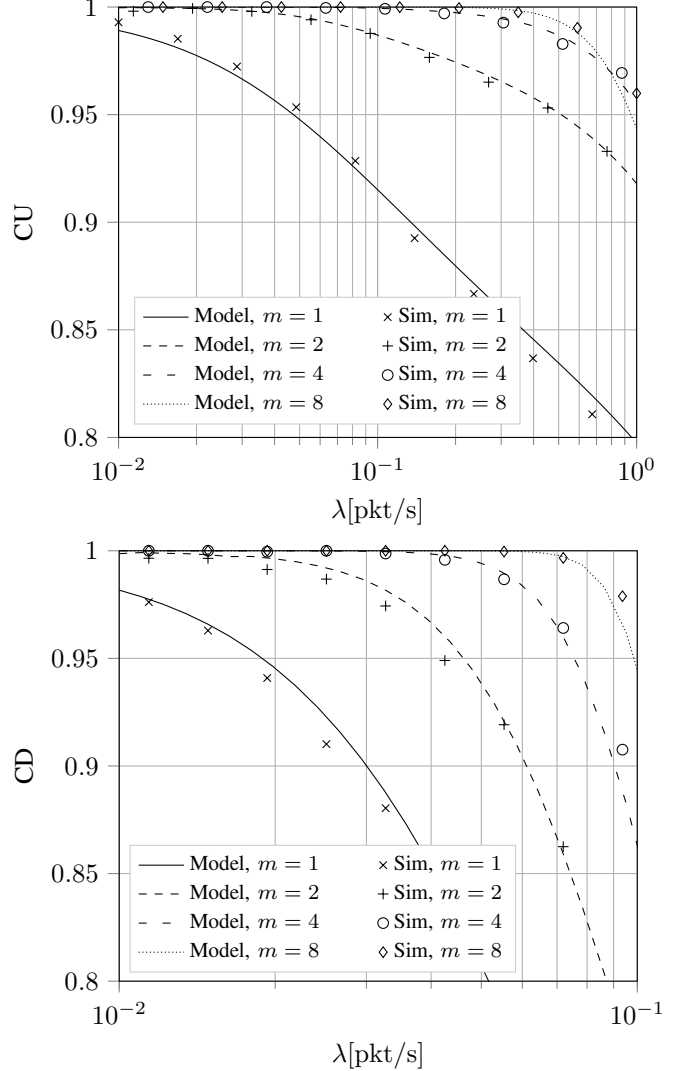


Figure 3. Comparison of model and simulation results in terms of CU and CD.

generate confirmed traffic ($\alpha = 0$), and for different values of m . The model results are quite close to those given by the simulations in the area of interest, where success probabilities are above 0.8. We can see that the increase in the number of available transmissions helps the correct delivery of the message at the MAC layer, providing performance above 0.9 also for relatively high traffic levels, when one packet per second is generated by the EDs at the application layer. The CD performance is much lower because the generation rate of DL messages is limited by the DC restrictions.

Fig. 4 compares simulation and theoretical results, in terms of both CU and CD, when different fractions of confirmed traffic are employed in the network. For this comparison, we set the application layer packet arrival rate to $\lambda = 0.1$ pck/s, and the maximum number of transmissions to $m = 4$. We can see that, as the fraction of EDs employing confirmed traffic increases, the performance decreases for all the EDs, in particular those that do not re-transmit their packets. We can

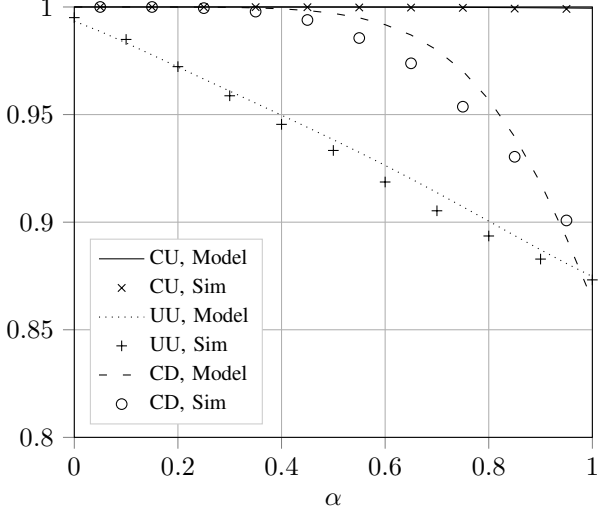


Figure 4. Performance when varying the fraction of confirmed traffic, with $\lambda = 0.1, m = 4$.

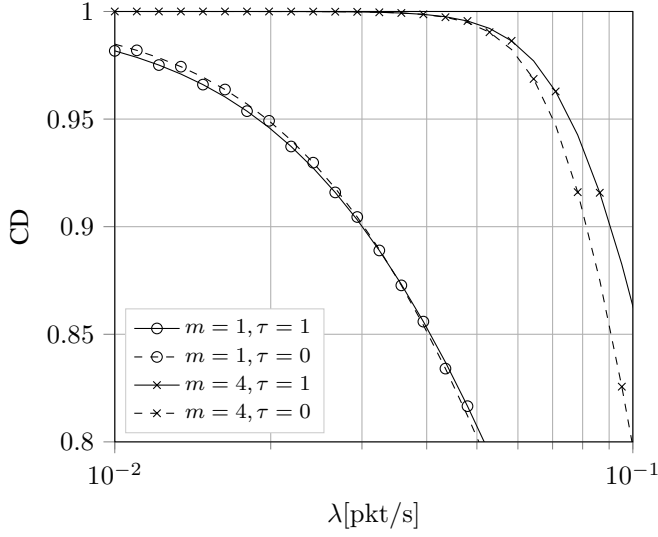


Figure 5. CD performance when varying TX/RX prioritization, obtained with $\alpha = 1$.

also observe some trade-offs between the system performance and the type of traffic that can be generated by the EDs, implying that if a certain level of performance is desired, the number of devices employing confirmed traffic must be limited. Additionally, increasing m to improve communication reliability yields worse performance for unconfirmed traffic because of interference and GW occupancy.

In Fig. 5 the model is used to verify the impact of RX or TX prioritization on the CD performance metric. It is interesting to see that, in a scenario where devices transmit at most once ($m = 1$), prioritizing RX is the best choice. Conversely, when re-transmissions are allowed, prioritizing TX yields the best results since the GW will give priority to the transmission of ACKs, thus blocking further retransmissions of UL packets.

Another example of how the model can be used to extract

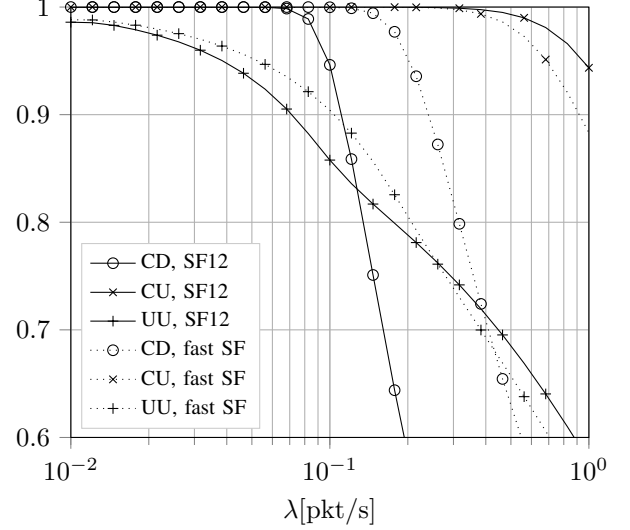


Figure 6. Performance when varying the SF of ACKs with $\alpha = 1$ and $m = 8$.

non-intuitive results is provided in Fig. 6, which shows the performance metrics in a network with $m = 8$ and $\alpha = 1$, when varying the policy used to set the SF of ACKs sent in RX2. In particular, beside the standard setting, which fixes SF to 12, we consider a “fast SF” configuration in which the ACK is transmitted using the same SF of the corresponding UL packet. The CD curve exhibits a gain in performance due to the fact that shorter DL messages in RX2 imply shorter DC banning periods, improving the availability of the GW to serve more devices in the same time frame.

The effect on the uplink metrics is instead more interesting: the UU improves for lower values of λ , and worsens for higher values of λ . The CU, instead, exhibits a degradation that is coherent with what was observed in the simulation study in [20]. This behavior is explained considering the DC regime of the GW: while, at low traffic rates, the GW is not affected by the limits imposed by the DC, at higher values of λ the DL pressure on the GW is such that the device will always have an ACK packet to transmit. These two very different contexts, in turn, affect the events at the PHY layer when the fast SF is employed in RX2: for lower λ values, fewer UL packets are lost due to GW transmissions, since ACKs take a shorter transmission time, leading to an increase in UU. When traffic grows and the fast SF is used, however, this positive effect is countered by the absence of the long stretches of silence the GW was forced to observe when employing SF 12, during which it could receive more UL packets. In other words, higher traffic rates lead to frequent short packet transmissions by the GW, which is worse for the uplink PDR metrics. These considerations are validated by the fact that, when DC is disabled, both CU and UU increase with the fast SF option, with respect to the baseline case where SF 12 is employed, even for high values of λ .

VII. CONCLUSION

In this work, we presented a model for the performance evaluation of a LoRaWAN network in the presence of both

confirmed and unconfirmed traffic, also taking into account the influence of different settings of multiple network configuration parameters.

In order to describe this chain of events we introduced a mathematical model, which is able to both capture the UL traffic performance and describe the multiple events that affect the outcome of the DL transmission: DC constraints, ongoing transmissions and receptions, and interference. We validated the model against simulation results. Even if the simulator considers aspects that are neglected in the model for tractability, the results of the model are representative of the network performance in all the settings that were tested. Finally, we showed some examples of how the model can be employed to analyze, with minimum effort, the effects of possible changes to the standard parameters configuration.

In future, we plan to extend the model to multi-GWs scenarios, where UL packets are potentially received by several GWs. Moreover, we plan to leverage the proposed model to optimize network parameters in different scenarios, or when specific performance requirements are provided.

ACKNOWLEDGMENT

Part of this work was supported by MIUR (Italian Ministry for Education and Research) under the initiative "Departments of Excellence" (Law 232/2016).

REFERENCES

- [1] A. Zanella, N. Bui, A. Castellani, L. Vangelista, and M. Zorzi, "Internet of things for smart cities," *IEEE Internet of Things Journal*, vol. 1, no. 1, pp. 22–32, Feb 2014.
- [2] Y. Yuehong, Y. Zeng, X. Chen, and Y. Fan, "The internet of things in healthcare: An overview," *Journal of Industrial Information Integration*, vol. 1, pp. 3–13, 2016.
- [3] N. Dlodlo and J. Kalezhi, "The internet of things in agriculture for sustainable rural development," in *2015 International Conference on Emerging Trends in Networks and Computer Communications (ETNCC)*, May 2015, pp. 13–18.
- [4] D. Croce, M. Guicciardo, S. Mangione, G. Santaromita, and I. Tinnirello, "Impact of LoRa Imperfect Orthogonality: Analysis of Link-Level Performance," *IEEE Communications Letters*, vol. 22, no. 4, pp. 796–799, 2018.
- [5] Semtech Corporation, *SX1301 datasheet*, 2014.
- [6] M. Capuzzo and D. Magrin and A. Zanella, "Confirmed traffic in LoRaWAN: Pitfalls and countermeasures," in *Annual Mediterranean Ad Hoc Networking Workshop (Med-Hoc-Net)*, Jun. 2018.
- [7] F. Van den Abeele, J. Haxhibeqiri, I. Moerman, and J. Hoebeke, "Scalability Analysis of Large-Scale LoRaWAN Networks in ns-3," *IEEE Internet of Things Journal*, vol. 4, no. 6, pp. 2186–2198, 2017.
- [8] B. Reenders, Q. Wang, and S. Pollin, "A LoRaWAN module for ns-3: implementation and evaluation," in *Proceedings of the 10th Workshop on ns-3*, Jun. 2018.
- [9] A. I. Pop, U. Raza, P. Kulkarni, and M. Sooriyabandara, "Does Bidirectional Traffic Do More Harm Than Good in LoRaWAN Based LPWA Networks?" in *IEEE Global Communications Conference (GLOBECOM)*, Dec. 2017.
- [10] N. Varsier and J. Schwoerer, "Capacity limits of LoRaWAN technology for smart metering applications," in *IEEE International Conference on Communications (ICC)*, May 2017.
- [11] F. Adelantado, X. Vilajosana, P. Tuset-Peiro, B. Martinez, J. Melia-Segui, and T. Watteyne, "Understanding the Limits of LoRaWAN," *IEEE Communications Magazine*, vol. 55, no. 9, pp. 34–40, 2017.
- [12] O. Georgiou and U. Raza, "Low Power Wide Area Network Analysis: Can LoRa Scale?" *IEEE Wireless Communications Letters*, vol. 6, no. 2, pp. 162–165, 2017.
- [13] J. Toussaint, N. E. Rachkidy, and A. Guitton, "Performance analysis of the on-the-air activation in LoRaWAN," in *IEEE Annual Information Technology, Electronics and Mobile Communication Conference (IEMCON)*, Oct. 2016.
- [14] T. Bouguera, J.-F. Diouris, J.-J. Chaillout, R. Jaouadi, and G. Andrieux, "Energy Consumption Model for Sensor Nodes Based on LoRa and LoRaWAN," *Sensors*, vol. 18, no. 7, p. 2104, 2018.
- [15] R. B. Sorensen, D. M. Kim, J. J. Nielsen, and P. Popovski, "Analysis of Latency and MAC-Layer Performance for Class a LoRaWAN," *IEEE Wireless Communications Letters*, vol. 6, no. 5, pp. 566–569, 2017.
- [16] D. Bankov, E. Khorov, and A. Lyakhov, "Mathematical model of LoRaWAN channel access with capture effect," in *IEEE Annual International Symposium on Personal, Indoor, and Mobile Radio Communications (PIMRC)*, Oct. 2017.
- [17] —, "LoRaWAN Modeling and MCS Allocation to Satisfy Heterogeneous QoS Requirements," *Sensors*, vol. 19, no. 19, p. 4204, 2019.
- [18] M. Capuzzo, D. Magrin, and A. Zanella, "Mathematical Modeling of LoRa WAN Performance with Bi-directional Traffic," in *IEEE Global Communications Conference (GLOBECOM)*, Dec. 2018.
- [19] D. Magrin, M. Centenaro, and L. Vangelista, "Performance evaluation of LoRa networks in a smart city scenario," in *IEEE International Conference on Communications (ICC)*, May 2017.
- [20] D. Magrin, M. Capuzzo, and A. Zanella, "A Thorough Study of Lorawan Performance Under Different Parameter Settings," *IEEE Internet of Things Journal*, 2019. [Online]. Available: <https://doi.org/10.1109/iot.2019.2946487>
- [21] C. Goursaud and J. M. Gorce, "Dedicated Networks for IoT: PHY / MAC State of the Art and Challenges," *EAI Endorsed Transactions on Internet of Things*, vol. 1, no. 1, p. 150597, 2015.